Journal of Biomedical Optics 7(1), 14–19 (January 2002)

# Laser activated fluorescence measurements and morphological features: an *in vivo* study of clearance time of fluorescein isothiocyanate tagged cell markers

**I. Gannot**
Tel-Aviv University
Department of Biomedical Engineering
Faculty of Engineering
Tel-Aviv 69978, Israel

**G. Gannot**
Tel-Aviv University
School of Dental Medicine
Department of Oral Pathology
Tel-Aviv 6978, Israel

**A. Garashi**
Tel-Aviv University
Department of Biomedical Engineering
Faculty of Engineering
Tel-Aviv 69978, Israel

**A. Gandjbakhche**
National Institutes of Health
National Institute of Child Health and Human Development
Unit on Biomedical Stochastic Physics
Laboratory of Integrative and Medical Biophysics
Bethesda, Maryland 20892

**A. Buchner**
Tel-Aviv University
School of Dental Medicine
Department of Oral Pathology
Tel-Aviv 6978, Israel

**Y. Keisari**
Tel-Aviv University
School of Medicine
Department of Human Microbiology
Tel-Aviv 69978, Israel

**Abstract.** Fourteen BALB/c mice were divided into two groups. One group served as the control and the second group was injected with a squamous cell carcinoma cell line to the tongue. After tumor development (1–4 weeks), mice were injected with a FITC conjugated CD3 marker to their tongues. Immediately after the marker injection, the clearance of the marker was measured using a laser spectroscopy system. The markers were excited by an argon laser at 488 nm and the fluorescence signal was measured as a function of time. A biopsy was taken from every mouse after the procedure and the excised tissue was histologically evaluated. Analysis of clearance times revealed a second order exponential decay for both groups with a slower pace of signal clearance for the sick mice.  [DOI: 10.1117/1.1427913]

Keywords: lasers; fluorescence; tissues.

Paper JBO-102105 received Apr. 12, 2001; revised manuscript received Aug. 20, 2001; accepted for publication Sept. 25, 2001.

## 1 Introduction

Various optical diagnostic methods are in different stages of their development. Among them are optical coherence tomography,[1] optical tomography,[2] polarization imaging,[3] optoacoustics,[4] autofluorescence based imaging,[5] and others. Each method is based on a different principle of operation and fits to various depths and structures. When looking deep under the tissue surface, endogenous properties of tissues are not enough. There is a need to enhance the signals coming from atypical sites in tissue with exogenous markers, which will be applied by different means. These should be markers with a specific affinity to tissues that are to be examined. The most appropriate marker to use is the antibody that recognizes specific sites on tissues and is biocompatible to the body. The antibodies are also conjugatable to markers that can be excited by a laser source. The mathematical reconstruction of the location and concentration of the foci is developed by an NIH group[6] and some aspects in collaboration with us[7] as well as by other research teams.[8] In this paper we will not deal with this issue.

Many of the parameters affect the clearance time and behavior of applied fluorophores to examined tissue. From the biological point of view several issues of importance can be listed, i.e., the physical status of the subject under investigation (anesthetized or in full activity), the pathological condition of the tissue (such as tumors or trauma), and the morphological features of the ''clearance vehicle,'' hence, the blood vessels (amount and size).[9,10]

Important parameters to consider are also the amount and concentration of the fluorophores injected to tissue, the type of fluorophore, and the type of the conjugated material to the fluorophore.

From the measurement point of view the main parameters include the laser source (energy and wavelength), spectral

Address all correspondence to I. Gannot. Tel: 972-3-6406711; Fax: 972-3-6407939; E-mail: gannot@eng.tau.ac.il

1083-3668/2002/$15.00 © 2002 SPIE

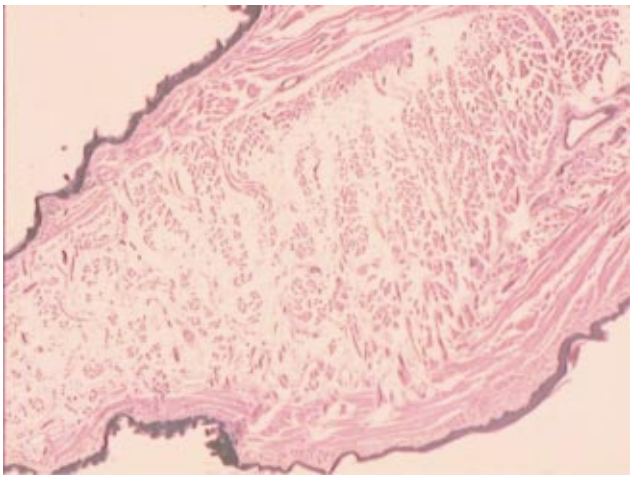

**Fig. 1** Normal tongue (healthy)—after the CD3–FITC injection. Magnification ×20. H&E staining.


**Fig. 2** Tongue injected with SqCC (sick)—after CD3–FITC injection. Magnification X20. H&E staining.

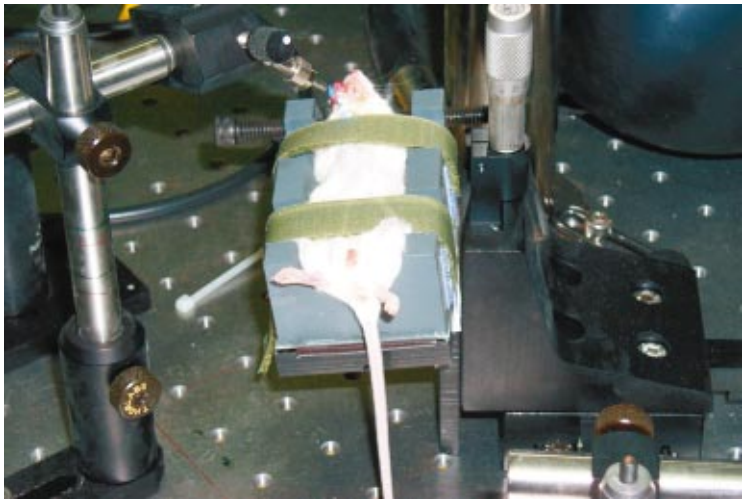

**Fig. 4** Mouse in specially designed holder.

**Fig. 6** Fluorescence signal from the mouse tongue.

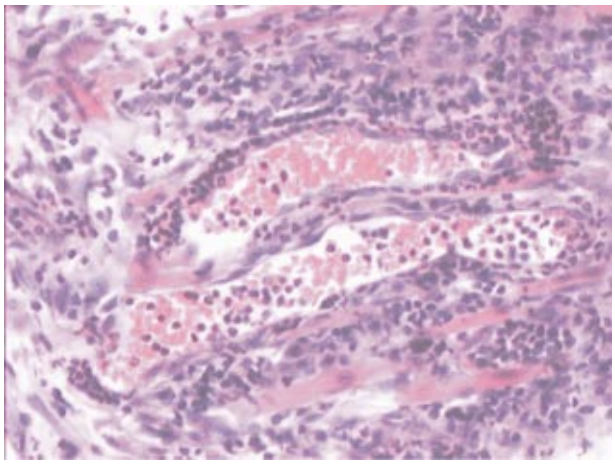

**Fig. 8** Blood vessels inside the tumor. H&E staining. Magnification ×200.

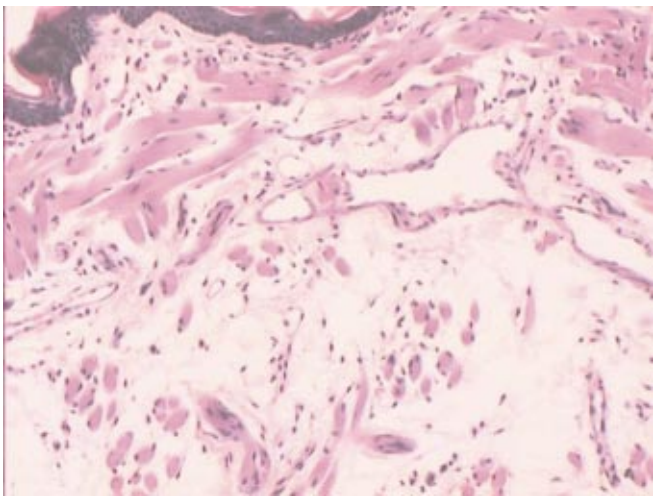

**Fig. 9** Blood vessels healthy tongue. H&E staining. Magnification ×100.

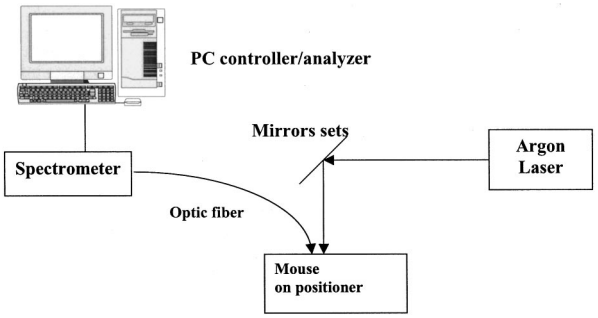


**Fig. 3** Experimental setup for measuring clearance time of fluorescent markers embedded in the mice tongue.

measurements (one or multidetectors), and fluorescence imaging system sensitivity.

In this paper we examined the correlation between tumor existence in the examined tissue (tongue) and clearance time of a fluourophore conjugated to antibodies as measured by laser excited spectral measurements. In the present study we worked with CD3–FITC conjugated antibodies. The FITC has an absorption peak at 488 nm (which fits an argon emission line). The CD3 antibody recognizes the CD3 positive cells in the tissues. These CD3 positive cells appear in an inflammation or when a tumor grows (data in a related paper to be published). These are the target cells in our study. This work is an initial step to establish guidelines for the measurements of laser-induced fluorescent imaging of exogenous fluorophores applied to tissue, as a mean to perform diagnosis of disease *in vivo*.

## 2 Materials and Methods

### 2.1 Cell Line

The squamous cell carcinoma cell line (SqCC) was established from a spontaneously developed squamous cell carcinoma in a BALB/c mouse skin. The cell line was maintained in sterile conditions in Dulbecco's modified eagle's medium

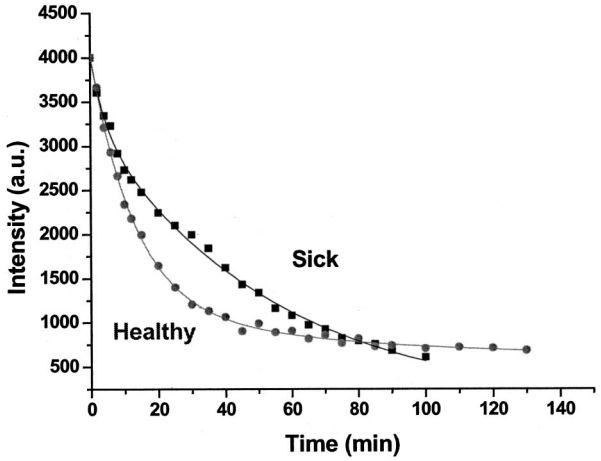


**Fig. 7** Unified clearance curves of healthy and sick mice.

(Biological Industries, Israel) supplemented with 10% fetal calf serum (Biological Industries, Israel), D-glucose 3500 mg/L (AnalaR, Israel), L-Glutamine 2 mM (Fluka, USA), and Penicillin 100 U/mL+streptomycin 100 $\mu$g/mL (Sigma, USA) solutions. The day of the injections cells were treated with Versene Trypsin solution (Sigma, USA), a final concentration of $10^5$ cells/50 $\mu$L in phosphate buffered saline (PBS) was established as the final concentration for injection.

### 2.2 Animals

Fourteen BALB/c mice were divided into two groups. One group (seven mice) served as the control and the second group was injected with SqCC into the tongue. Every mouse in the experimental group was injected with a volume of 50 $\mu$L cells in PBS. The control mice were injected with a media that the cell line was grown with (DMEM).

At various times after the cell line injection (1–4 weeks postcell line injection) the mice were anesthetized by using a mixture of 1 mL of imalgen/vetalar, (Ketaset, IO) and 250 mL of xylazin (Vitamed, Israel), in a total volume of 10 mL sa-

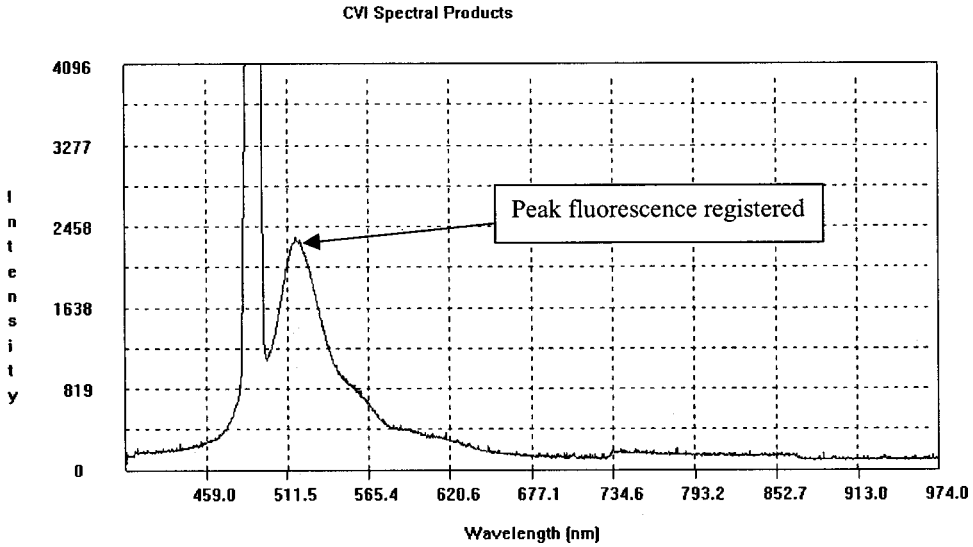


**Fig. 5** Fluorescence intensity signal dependence of wavelength. The fluorescence spectral range is between 515 and 600 nm.

line. Mice were injected with anti CD3–FITC antibodies (Southern Biotechnology, CA) in a volume of 50 $\mu$L into the tongue. Immediately after the injection the tongues were examined with the laser excited spectral measurement system. Right after the measurements (see details in next section) the tongues were excised, fixed in formalin, and embedded in paraffin. 4-$\mu$m-thick sections were prepared and stained with haematoxilin and eosin (H&E). Morphological features were identified. Figure 1 is an H&E staining of a section obtained from a healthy tongue and Figure 2 is a section from an injected tongue with a clear tumor formed in the middle of the tongue.

### 2.3 Optical Measurement System

The optical system set up is illustrated in Figure 3. It includes a continuous wave–30 mw argon laser (Spectra Physics, Mountain View, CA) emitting at 488 nm wavelength (optimized to the FITC absorption line). The laser beam was directed to the tissue through sets of reflecting mirrors. The fluorescence signal was measured by a PC controlled fiber optic spectrometer (SM240 spectrometer-CVI spectral product, Putnam, CT). The anesthetized mouse was held on a custom designed device (to avoid movement of the head) which was mounted on an *XYZ* positioner (Figure 4). The fluorescence was captured with an integration time, which covered at the beginning the maximum dynamic range of the system (app. 400 $\mu$s). At the beginning (for 16 min), the measurements were frequent (2 min apart) and with larger intervals thereafter (5 or 10 min between measurements). A sample of the fluorescence signal is shown in Figure 5. The fluorescence signal as it was detected on the mouse tongue is shown in Figure 6. The peak value of this signal was captured and exported to an EXCEL working sheet. Each measurement was done till the fluorescence signal became steady for a considerable amount of time or faded away totally. Measurements were done on healthy mice and sick mice at different stages of tumor development. The results were analyzed with ORIGIN software (Microcal, Northampton, MA).

## 3 Results and Discussion

The peak fluorescence from every mouse was captured as a function of time. Best-fit curves were calculated for each mouse. The results were averaged separately for each group. The unified curves are shown in Figure 7. These are second order exponential decay fits with 0.997 64 fit for the sick mice, and 0.998 71 fit for the healthy mice. Both are excellent fits.

These results show that the clearance of the fluorescinated marker conjugated to the CD3 antibody behaves the same way for the sick group and the healthy group. Since the results fit second order curves so well, it might be concluded that the clearing of the marker occurred in a two-step fashion. The first step was a fast clearing that was followed by a slower clearing of the signal. There were, however, changes in the pace of the signal clearance. While in the healthy controls, the marker reached the second step of clearance after 30 min; in the sick mice group it took almost 60 min for the signal to reach the second step of clearance (Figure 7). The extended retention of the antibody-FITC conjugate is not surprising since it is expected that the existence of the tumor will interfere with the normal clearing of the FITC marker though the tumor did not significantly change the clearance time nor the clearance behavior. This is due, in part at least, to the massive blood vessels formation (angiogenesis) inside the tumor, as is illustrated in Figure 8. Figure 9 shows the blood vessels in the normal tongue. Another parameter that influenced the retention of the CD3–FITC marker is the retention of this antibody by CD3 positive cells that become prominent in the tumor site as the tumor grew larger (data not shown).

These results are the initial step in a larger study in which we attempt to establish a noninvasive optical biopsy system. The final step in our research is to measure specific binding of the CD3 antibodies to the immune/inflammatory cells that infiltrate the tongue as the tumor grows. That was the initial reasoning for using this antibody in the present study. The signal obtained by the excitation of the FITC marker after the binding will indicate a state of health or disease. In the present work we have looked at the ''nonspecific'' clearance. This is the clearance of the access of the FITC marker that did not bind to the CD3 positive cells and is the ''noise'' in the system. This nonspecific staining masks the specific binding. We have shown that this clearance is longer in the sick mice.

## 4 Summary

The nonspecific clearance does not yet define the window of time where only specific binding is left. This may take several hours in mice and probably much longer when applied eventually to humans. The remaining signal (that consists mostly from the specific signal) was quite low which will force a much longer integration time to collect the fluorescence signals. This will cause some sensitivity problems that need to be solved. The next step in this study will be to use a multidetector array to cover a few angles to collect the fluorescent signals. Longer times between the injection and measurements will be taken. Another issue that will need to be taken into account is the location of the tumor in the tissue and how deep it is under the surface. At that situation the fluorescence signal intensity will be even lower. The dependence of the tumor size will be measured also. The tumor sizes which were used in the earlier described experiment was 1–2 mm.

The earlier experiment proves that when moving into *in vivo* measurements, a host of parameters needs to be considered before designing a reliable fluorescence biopsy method.

### Acknowledgments

The group wishes to thank the Ministry of Science, Technology, Culture and Sport for its support through the strategic research grant (Grant No. 8445) and the Binational Science foundation grant (Grant No. 1998308).

### References

1. J. M. Schmitt, ''Optical coherence tomography (OCT): A review,'' *IEEE J. Sel. Top. Quantum Electron.* **5**(4), 1205–1215 (1999).
2. S. R. Arridge, ''Optical tomography in medical imaging,'' *Inverse Probl.* **15**(2), 41–93 (1999).
3. S. G. Demos, A. J. Papadopoulos, H. Savage, A. Heerdt, S. Schantz, and R. R. Alfano, ''Polarization filter for biomedical tissue optical imaging,'' *Photochem. Photobiol.* **66**(6), 821–825 (1997).
4. R. O. Esenaliev, A. A. Karabutov, and A. A. Oraevsky, ''Sensitivity of laser opto-coustic imaging in detection of small deeply embedded tumors,'' *IEEE J. Sel. Top. Quantum Electron.* **5**(4), 981–988 (1999).
5. M. Hashimoto, Y. Takeda, T. Sato, H. Kawahara, O. Nagano, and M. Hirakawa, ''Dynamic changes of NADH fluorescence images and

NADH content during spreading depression in the cerebral cortex of gerbils,'' *Brain Res.* **872**, 294–300 (2000).
6. A. H. Gandjbakhche and G. Weiss, ''Random walk and diffusion like model for photon migration in turbid media,'' *Prog. Opt.* **34**, 333–402 (1995).
7. I. Gannot, R. F. Bonner, G. Gannot, P. C. Fox, P. D. Smith, and A. H. Gandjbakhche, ''Optical simulations of a noninvasive technique for the diagnosis of diseased salivary glands *in situ*,'' *Med. Phys.* **25**(7), 1139–1144 (1998).
8. D. E. Hyde, T. J. Farrell, M. S. Patterson, and B. C. Wilson, ''A diffusion theory model of spatially resolved fluorescence from depth-dependent fluorophore concentrations,'' *Phys. Med. Biol.* **46**, 369–383 (2001).
9. S. Calatayud, M. D. Barrachina, E. Garcia-Zaragoza, H. Mattsson, J. V. Esplugues, ''Changes in gastric mucosal permeability induced by haemorrhagic shock in the anaesthetized rat: modulation by acid,'' *J. Pharm. Pharmacol.* **50**(10), 1095–1100 (1998).
10. Y. Kaneo, T. Uemura, T. Tanaka, S. Kanoh, and A. Matsuoka, ''Pharmacokinetics of glutathione-dextran macromolecular conjugate in mice,'' *Biol. Pharm. Bull.* **18**(11), 1544–1547 (1995).